Journal of Engineering Science and Technology
Vol. 16, No. 5 (2021) 3866 - 3879


# FRESNEL LENS SOLAR CONCENTRATOR TO UTILIZE THE EXTREME SOLAR INTENSITY IN HEAT EXCHANGER RECEIVERS

AHMED H. OBAID[1,*], ASSAAD AL SAHLANI[1], ADEL A. EIDAN[2]

[1]Al-Furat Al-Awsat Technical University, Engineering Technical College of Al-Najaf, 31001, Iraq
[2]Al-Furat Al-Awsat Technical University, Najaf Technical Institute, 31001, Iraq
*Corresponding Author: ahmed.mm9696@gmail.com

## Abstract

This work presents an experimental study of water heating using heat exchanger receivers with a fresnel lens concentrator. Two models of the heat exchangers are used, namely conical pipe and cubical tank heat exchangers, to investigate the thermal efficiency of different models. Each heat exchanger is resided at the focus of the fresnel lens, where the fresnel lens concentrator is controlled to track the solar light and maintain the focal stationery. The results showed that the highest thermal efficiency was recorded for the conical pipe heat exchanger where the efficiency was 30% when the intensity of the solar radiation was 1159 W/m$^2$ and the ambient temperature was 16°C. Whereas the highest thermal efficiency of the cubical tank heat exchanger was 26% when the intensity of the solar radiation was 1197W/m$^2$ and the ambient temperature was 21°C. Also, the results showed that the fresnel lens concentrator can be efficiently used to provide hot water during wintertime under Iraqi weather.

Keywords: Fresnel lens, Solar energy, Solar tracking system.

## 1. Introduction

The increasing demand for energy, generated by power plants that use fossil fuels, has consequences on traditional fuel resources, which are under constant depletion, and the climate changes resulting from emissions from fossil fuel combustion. Green energy is the most promising source of renewable energy, as its solar energy can be invested in several ways. For example, solar radiation can be captured by solar thermal collectors, which produce thermal energy used in heating water for domestic or industrial applications. Several studies have been done to investigate the effectiveness of a different type of receiver with a solar concentrator, yet only a limited number have been mentioned in the literature that examined the effect of using different types of receivers with a fresnel lens concentrator.

Zou et al. [1] investigated a special parabolic trough collector, to heat water in cold areas. The PTC consists of a parabolic shape with a reflector mirror surface and a receiver tube at the concentrator's focal line. The result showed that the thermal efficiency of the PTC was 67% even under solar radiation conditions below 310W/m$^2$. In a similar manner, Bakos et al. [2] used a parabolic trough collector for steam generation. The system was capable of tracking the daily path of the sun. The results showed that the efficiency of the PTC is a function of the pipe length, the diameter of the pipe, the intensity of the solar radiation, and the heat transfer fluid flux. On the other hand, Palavras and Bakos [3] developed the characteristics of a satellite dish solar concentrator, which equipped with a polymer mirror as a solar reflective surface. The dish solar concentrator was connected to a solar tracking system. The system produced a temperature of more than 300°C in the focus. Sakhare and Kapatkar [4], investigated the idea found by Palavras and Bakos [3] by using a parabolic dish collector for water heating and cooking. The collector is fabricated with aluminum foil as a reflective material and using a receiver of a helical copper tube, it is mounted at the focus of the collector. The results showed that the temperature of the coil receiver is 190°C. Similarly, Mohammed [5] developed a parabolic dish for solar water heater, which used for domestic hot water use (up to 100°C) is defined. The used automatic electronic control circuit for the architecture of the solar water heater keeps track of the sun continuously. Experimental test runs have shown that the total output of the solar water heater was a thermal efficiency of 52%-56%.

Another device to manufacture solar concentrators was introduced by Al-Dohani et al. [6] who developed a fresnel lens to generate steam and electricity. The device consists of a fresnel lens with a heat exchanger. In the focal point of the fresnel lens the resulting solar heat is absorbed in the heat exchanger and the molten salt is melted and the heat is transferred to the water. This produces steam, and the resulting steam is used to spin the engine along with a generator. The maximum power output of 30W was produced at 700W/m$^2$. The use of the lens was enlarged by Valmiki et al. [7] who presented a fresnel lens as a prototyped solar cooking stove useful for solar cooking and heating. The stove has a fixed heat-region at the focal point of the lens which the solar tracking device rotates the lens around its focal point. The results showed the possibility of obtaining temperatures up to 300°C on the stovetop surface. The heat can be used for cooking and internal heating. Moreover, Tripanagnostopoulos et al. [8] used linear glass type fresnel lenses to control lighting and building temperature. The fresnel lens focuses part of the solar radiation that passes through it in the receiver in the focus and leaves rest to distribute in the building for lighting or uses the photovoltaic/thermal absorbers to produce heat, electricity, or both. When using the proposed system to cool the building area, the results showed a satisfactory temperature drop in excess of 10°C. Lin et al. [9] investigated the linear fresnel lens solar collector with different forms of cavity receiver (triangular, arc cavity, rectangular and semi-circular). The experimental and numerical methods are used to obtain the optimum optical and thermal performance. Results showed that the use of the fresnel lens concentrator with a triangular cavity receiver has a better optical and thermal performance (81.2% and 30% at 120°C respectively) another form of a receiver. Soriga and Neaga [10] used a linear fresnel lens solar collector with a cylindrical cavity receiver. The receiver is formed by a copper tube inside a vacuum glass tube. The results showed that the design parameters in addition to the effect of the environmental and operational factors on the performance of the collector. It also showed that a higher efficiency value for the fresnel lens concentrator was observed as compared to the (CPC) with the same type of receiver. Nia et al. [11] presented a thermoelectric application where a fresnel lens concentrator produces electric power during on-sun operation.

The aim of the work is to generate electricity and heated water, electricity is generated as a result of the heat transfer through the (TE) module. The results showed the generation of power is 1.08W with 51.33% efficiency when the intensity of the solar radiation 705.9W/m$^2$. Perini et al. [12] presented a number of a PMMA fresnel lens solar collectors with a heat transfer model receiver pipe. The aim of the research is to determine the efficiency curve of the collector using the method of experimental and theoretical analysis. The results showed that the efficiency of the collector is limited to less than 20%. The reason for the lower efficiency is the loss of energy due to the optical loss in the lens and the low solar absorption of the receiver pipe. Xie et al. [13] investigated the fresnel lens solar collector with different configurations of cavity receiver (conical, cylindrical, and spherical receiver) equipped with a two-axis tracking mechanism. To easily compare the thermal output of the fresnel solar collector using different point-focus cavity receivers. The result showed that among the three type's receivers, the best shape was the cone receiver, which has the highest thermal efficiency and the lowest heat loss.

This work presents an experimental study about using fresnel lens solar concentrator to utilize the extreme temperature at the focal of the concentrator to produce hot water under Iraqi weather and this paper is organized as follows; section 2 illustrates the experimental rig setup, and section 3 contains the experimental results and discussion and finally, the concluding remarks are in section 4.

## 2. Experimental Setup

The experimental rig consists of two main parts, namely the solar concentrator and the sun tracking control part as follows:

### 2.1. Fresnel lens solar concentrator

The solar concentrator is a mechanism that allows a two-axis free motion to track the sun during daylight. The fresnel lens is to be mounted using a frame such that the concentrating focus stays stationary during the motion holding frame. A square fresnel lens with the following specification is used (dimensions: 520 x 520mm, focal length: 620mm, thread distance: 0.5mm, thickness: 3mm, material: optical PMMA). Figure 1 illustrates the details of the solar concentrator components.

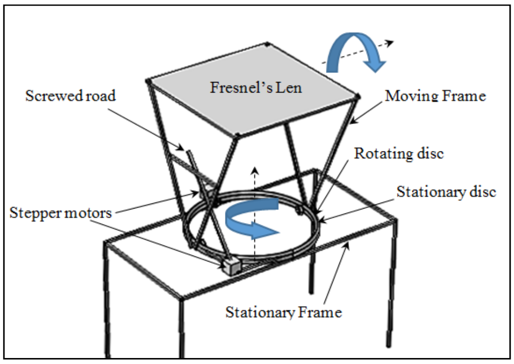

**Fig. 1. Experimental setup and schematic diagram of the fresnel lens solar concentrator.**

## 2.2. Sun tracker control system

The sun path can be tracked efficiently by sensing sunlight to specify the position of the sun. Another way to track the sunlight efficiently is to calculate the sun's position in the sky via calculation of azimuth and altitude angles for a given region, time and date. In this work, the second approach is used. Where a control system is implemented to track the sunlight. The control system consists of a controlling circuit represented by an Arduino unit and two stepper motors to apply the motion to the tracking frame, one motor to move the frame vertically and the other one is to rotate the circular base horizontally. The Arduino unit is programmed such that the altitude and azimuth angles are calculated simultaneously based on the given date and time. The control system is initiated by feeding the date and time beforehand, we implemented this solar and tracking system in our previous work [14]

The position of the sun at a given time may be measured at a specific location of known latitude and longitude. The celestial coordinates needed to determine its position for a given location on Earth are the solar altitude angle, ($\alpha$) and the solar azimuth angle ($Z$). The time involved in the apparent solar time ($AST$) to express the time of day for a given area, which defines the exact time of the sun in relation to the local time, and is given by [15]:

$$AST = LST + ET \pm 4(SL - LL) \quad (1)$$

$$ET = 9.87 \sin(2B) - 7.53 \cos(B) - 1.5 \sin(B) \quad (2)$$

$$B = \frac{(N-81)360}{364} \quad (3)$$

where $LST$ is the local standard time, $SL$ is the standard longitude, $LL$ is the local longitude, and the $ET$ is the equation of time in minutes and is given by Eq. 2. From Eq. 3, $N$ is the day of the year, and if the location is east of Greenwich, the sign of Eq. 1 is minus (-), and if it is west, the sign is plus (+). The solar altitude angle ($\alpha$) and solar azimuth angle ($Z$) are calculated mathematically for each month, day, and hour of the year using Eq. 4 and 5 [15]:

$$\sin(\alpha) = \sin(L)\ \sin(\delta) + \cos(L) \cos(\delta) \cos(h) \quad (4)$$

$$sin(Z) = \frac{cos(\delta) sin\,(h)}{cos(\alpha)} \quad (5)$$

$$\delta = 23.45\,sin\left[\frac{(284+N)360}{365}\right] \quad (6)$$

$$h = \pm 0.25 \text{ (Number of minutes from local solar noon)} \quad (7)$$

where $L$ is the local latitude, $\delta$ is the solar declination angle, $h$ is the hour angle. The sign in Eq. 7 is plus (+) applies to afternoon hours and the sign is minus (-) to morning hours. The position of the sun is calculated at any time for a specific location on the earth through the angles of solar altitude angle ($\alpha$) and solar azimuth angle ($Z$). After calculating the two angles, solar altitude angle ($\alpha$) and solar azimuth angle ($Z$), that define the position of the sun in the sky by using the above equations. The $\alpha$ and $Z$ angles are calculated for each day, hour, minute of the year. The Arduino unit is programmed such that the altitude and azimuth angles are calculated simultaneously based on the given date and time, as shown in Fig. 2. The signals received from the control system unit are used to control the operation of the first motor to rotate the lens on the horizontal axis, and to rotate the second motor to rotate the lens on the vertical axis.

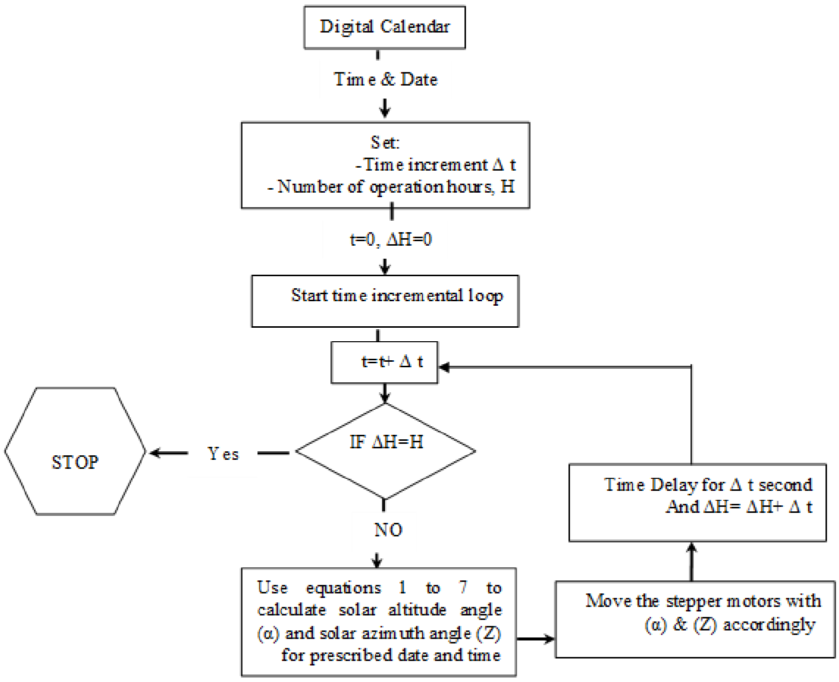


## 2.3. Heat exchanger receivers

Two models of the heat exchanger receivers are manufactured and tested. The models are conical pipe and cubical tank heat exchangers; both models are used to capture the concentrated thermal energy in the focus. The conical pipe heat exchanger consists of a copper tube with a diameter of 5mm, twisted in a conical shape with an aperture of an upper diameter of 10cm, a lower diameter of 4cm, and a height of 10cm, as shown in Fig. 3(a). The outside of the conical pipe is covered by an aluminium plate with a thickness of 1mm. Both of the conical pipe and the aluminium plate are placed in an aluminium the cylindrical container. The receiver is isolated from the surrounding by filling the space between cylindrical container and the aluminium plate with polyurethane foam, to reduce the thermal loss by convection with ambient.


**(a) Conical pipe heat exchanger.**

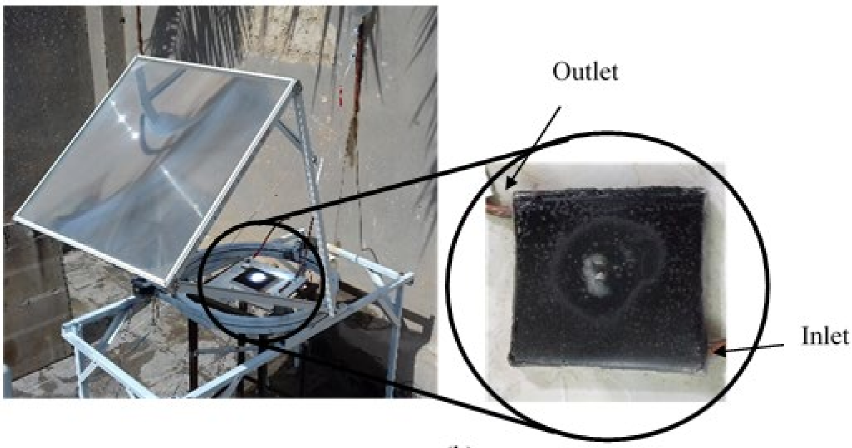


**(b) Cubical tank heat exchanger.**

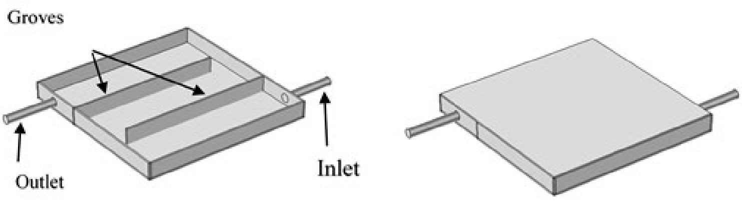


**(c) Cubical tank heat exchanger.**

**Fig. 3. Heat exchanger receivers' model.**

The second model is the cubical tank heat exchanger which consists of an aluminum tank of a height of 1cm, a length of 10cm, and a width of 10cm, as shown in Fig. 3(b). The heat exchanger provided with a number of internal grooves to circulate the water flow inside the tank, as shown in Fig. 3(c). The model is painted black to increase the absorption of solar radiation. The collector thermal efficiency (Ƞ) was calculated by the following equation [13]:

$$\eta = \frac{m\,Cp(To - Ti)}{I\,A} \quad (8)$$

where $m$ is the mass flow rate of the heat transfer fluid, $Cp$ is the specific heat of the fluid at the outlet temperature, $T_i$ is the fluid inlet receiver temperature, $T_o$ is the fluid outlet receiver temperature, $I$ is the direct solar radiation and $A$ is the area of the fresnel lens. The temperature of the water inlet and outlet was measured using thermocouples type-K. It has a wide range of measuring temperatures from (-270 to 1260)°C. Thermocouples are joined with data logger temperature modal Applent 32 channels temperature recorder for heating appliance (AT4532) with measurement range (-200 - 1300)°C and accuracy 0.2% + 1°C. The direct solar radiation reached on a fresnel lens was measured using (Tenmars TM-207 Solar Power Meter)W/m$^2$. It has a range to measure solar intensity from (0 to 2000)W/m$^2$; the accuracy of solar irradiation is (± 0.5%).

## 2.4. Uncertainty

It is crucial to investigate the system uncertainties since this is an experimental study. The well-known method presented by Abernethy et al. [16] was used to calculate the system uncertainties by accumulating up the uncertainty of each system element of the experimental setup. The system uncertainties of the present work were found to be in the range of 2.5% and it was calculated by the following formula.

## 3. Results and Discussion

The experimental tests are performed with local weather condition in Najaf city/Iraq (44°E, 31°N) [17]. Two models of heat exchangers are used, namely conical pipe and cubical tank heat exchangers. In total, the study included six experiments. For the conical pipe heat exchanger, the experiments were performed three times in three consecutive days with different water flow rates (1, 2 and 4 litres per hour, respectively), and a similar procedure was followed for the cubical tank heat exchanger. The data was collected using two thermocouples type-K that are installed on the inlet and outlet pipes of the receivers. The temperature measurement is recorded by means of a digital data logger and the experiments are performed as follows:

## 3.1. Conical pipe heat exchanger

Practical experiments were conducted during the period 13th to 15th of February 2020 from 9 am to 3 pm, where the ambient temperature ranged from 8°C to 19°C and the solar radiation ranged from 950W/m$^2$ to 1353W/m$^2$, as shown in Fig. 4.

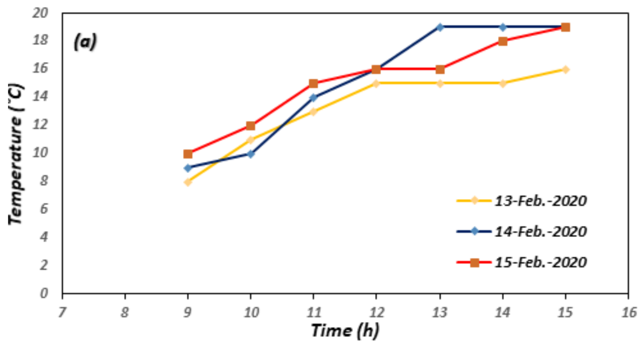


**(a) Ambient temperature versus time.**

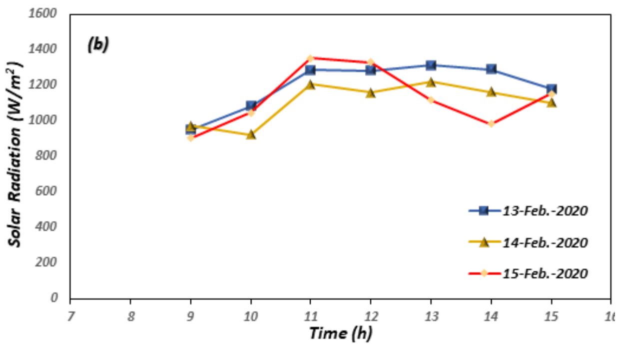


**(b) Solar radiation versus time.**

**Fig. 4. Climatic conditions under which the experiments have been conducted of conical pipe heat exchanger.**

Figure 5(a) shows the relation between the temperature of water inlet, outlet, and thermal efficiency versus time for the conical pipe heat exchanger at water flow rate was 2 *L*/*h* during the 13th of February, where the ambient temperature ranged from 8°C to 16°C and solar radiation in W/m$^2$ ranged from 950 to 1311. The average inlet water temperature is 14.2°C and the average water outlet temperature is 41°C. The efficiency of the conical tube heat exchanger was found to be in the range of 20 to 21%, and similar observation was reported by Perini et al. [12]

Figure 5(b) shows the relation between the temperature of water inlet, outlet and thermal efficiency versus time for the conical pipe heat exchanger at water flow rate was 4 *L*/*h* during the 14th of February, where the ambient temperature ranged from 9°C to 19°C and the solar radiation in W/m$^2$ ranged from 972 to 1220. The average inlet water temperature is 15.7°C and the average water outlet temperature is 32°C. Efficiency ranged from 25% to 30%, with an average of 28%.

Figure 5(c) shows the relation between the temperature of water inlet, outlet and thermal efficiency versus time for the conical pipe heat exchanger at water flow rate was 1 *L*/*h* during 15th of February, where the ambient temperature ranged from 10°C to 19°C and the solar radiation in W/m$^2$ ranged from 902 to 1353. The average inlet water temperature is 15°C and the average water outlet temperature is 71°C. Efficiency ranged from19% to 24%, with an average of 22%. Noting that at 14:00 the sky turned into partial cloudy resulting in a reduction in the amount of solar radiation to 982W/m$^2$, causing a decrease temperature of the water outlet to 69°C.

In experiments 1, 2, and 3, the main parameter investigated was the water flow rate, 2, 4, and 1 *L*/*h*, respectively. As previously mentioned, the experiments were performed on three consecutive days so that the other contributing parameters, such as ambient temperature and solar radiation, will be in the same range; for example, the minimum solar radiation was about 900's and the maximum solar radiation was about 1300's. The deference of the average temperature of water between outlet and inlet was 27, 17, and 56°C respectively, which reflects a decreased temperature as the flowrate increased. On the other hand, the efficiency increased with the increase of the flow rate, where the maximum efficiency was 30% with a flow rate of 4 *L*/*h*.

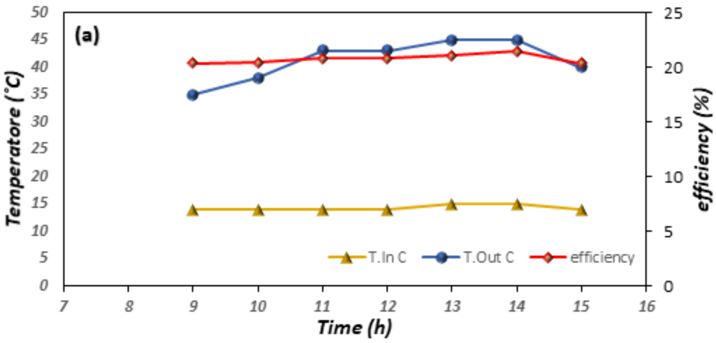


**(a) 2 *L*/*h*.**

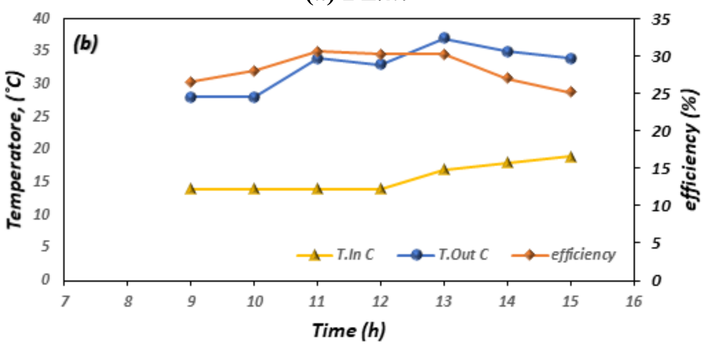


**(b) 4 *L*/*h*.**

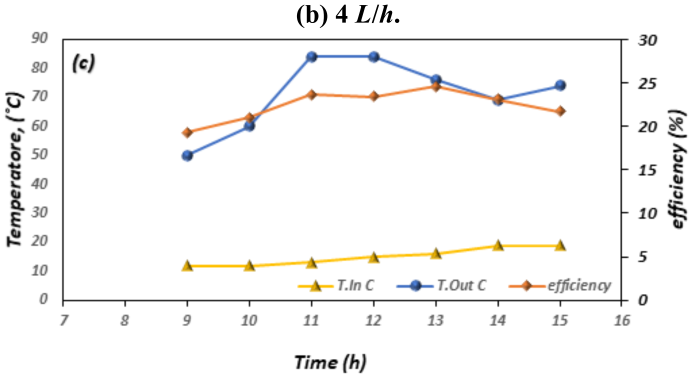


**(c) 1 *L*/*h*.**

**Fig. 5. Temperature of water inlet, outlet and thermal efficiency versus time of conical pipe heat exchanger.**

## 3.2. Cubical tank heat exchanger

Practical experiments were conducted during the period 22nd to 28th of February 2020 from 9 am to 3 pm, where the ambient temperature ranged from 15°C to 24°C and the solar radiation ranged from 855W/m$^2$ to 1387W/m$^2$, as shown in Fig. 6.

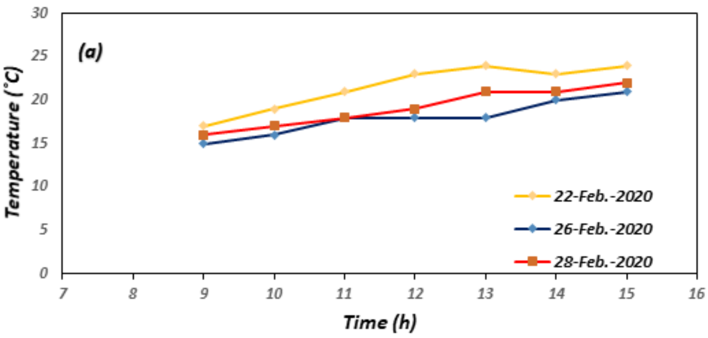


**(a) Ambient temperature versus time.**

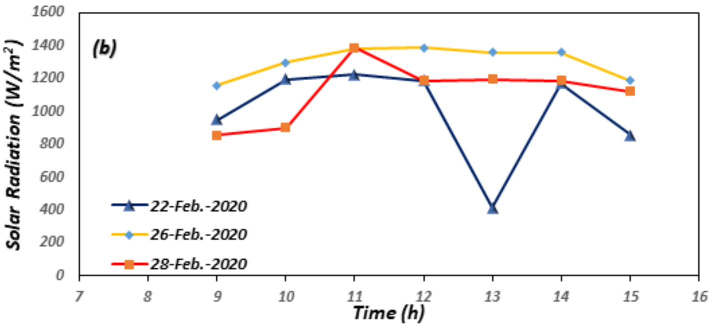


**(b) Solar radiation versus time.**

**Fig. 6. Climatic conditions under which the experiments have been conducted of cubical tank heat exchanger.**

Figure 7(a) shows the relation between the temperature of water inlet, outlet and thermal efficiency versus time for the cubical tank heat exchanger at water flow rate was 1 *L*/*h* during 22nd of February, where the ambient temperature ranged from 17°C to 24°C and the solar radiation in W/m$^2$ ranged from 950 to 1225 . The average inlet, outlet water temperatures and thermal efficiency are 16°C, and 58°C and 19% respectively. Noting that at 13:00 the sky turned into partial cloud resulting in a reduction in the amount of solar radiation to 412W/m$^2$, causing a decrease temperature of water outlet to 34°C.

Figure 7(b) shows the relation between the temperature of water inlet, outlet and thermal efficiency versus time for the cubical tank heat exchanger at water flow rate was 2 *L*/*h* during 26th of February, where the ambient temperature ranged from 15°C to 21°C and the solar radiation in W/m$^2$ ranged from 1159 to 1387. The average inlet, outlet water temperatures and thermal efficiency are 17.5°C, 50°C and 23% respectively.

Figure 7(c) shows the relation between the temperature of water inlet, outlet and thermal efficiency versus time for the cubical tank heat exchanger at water flow rate was 4 *L*/*h* during 28th of February, where the ambient temperature ranged from 17°C to 22°C and the solar radiation in W/m$^2$ ranged from 855 to 1387. The average inlet, outlet water temperatures and thermal efficiency are 18°C, 33°Cand 24% respectively.

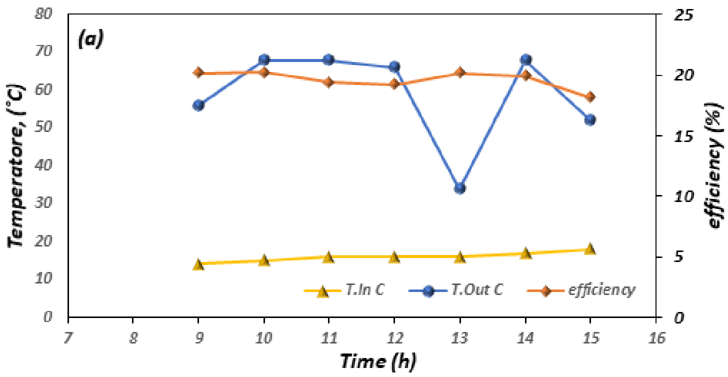


**(a) 1 *L*/*h*.**

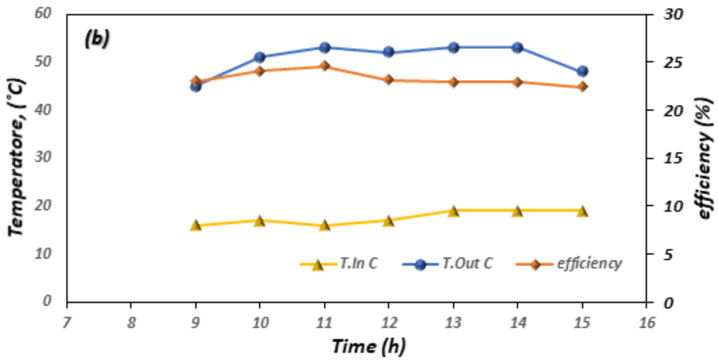


**(b) 2 *L*/*h*.**

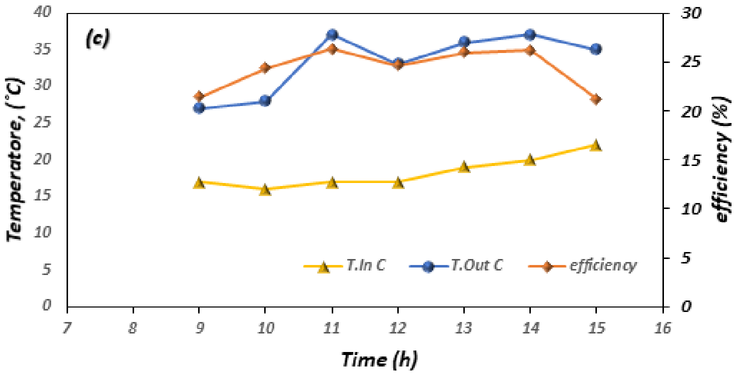


**(c) 4 *L*/*h*.**

**Fig. 7. Temperature of water inlet, outlet and thermal efficiency versus time of cubical tank heat exchanger.**

In experiments 4, 5, and 6, the main parameter investigated was the water flow rate, 1, 2, and 4 *L*/*h*, respectively. As previously mentioned, the experiments were performed on three consecutive days so that the other contributing parameters, such as ambient temperature and solar radiation, will be in the same range. The deference of average temperature of water between outlet and inlet was 42, 33 and 15°C respectively, which reflects a decreased temperature as the flowrate increased. On the other hand, the efficiency increased with the increase of the flow rate, where the maximum efficiency was 26% with a flow rate of 4 *L*/*h*. Comparing to result of an experiment performed on conical pipe heat exchanger, the conical pipe heat exchanger shows higher efficiency. This fact can be attributed to two factors as follows; first the thermal conductivity of the conical pipe (copper) is higher than the thermal conductivity of the cubical box (aluminium). On the other hand, in the case of the cubical box, the focal of the solar concentrator was applied within small spot on the box surface which limits the effect of the heating area. Whereas, in the case of the conical pipe, the focal is distributed along the inclination of the vertical axis of the cone as can be seen in Fig. 3, which provides wider heating spot that covers the inner coils in which increases the thermal performance.

## 4. Conclusions

The intensive solar radiation is used in Najaf city-Iraq to heat water by means of a fresnel lens concentrator. The solar concentrator system consists of a sun tracker control system and fresnel lens concentrator frame as the frame moves freely in two axes to track the sun and focus the solar radiation on a heat exchanger. The tracking system consists of a control circuit represented by Arduino and two stepper motors to adjust the position of the fresnel's lens focal by moving the motors accordingly. The focus produced by the fresnel lens is to be maintained stationary at a fixed position to ensure continuous heat flow to the heat exchanger. Two models of heat exchangers are used, namely conical pipe and cubical tank heat exchanger. The test was carried out during the arbitrary days in February 2020 and the results showed that the highest thermal efficiency recorded for the conical pipe heat exchanger is 30% when the intensity of the solar radiation is 1159W/m$^2$ and the ambient temperature is 16°C. The highest obtained thermal efficiency of the cubical tank heat exchanger was 26% when the intensity of the solar radiation is 1197W/m$^2$ and the ambient temperature is 21°C. It is a promising idea for using fresnel lens to heat water in relatively low temperature.

**Nomenclatures**

| | |
|---|---|
| *AST* | Apparent solar time, min |
| *Cp* | Specific heat, J/kg °C |
| *ET* | Equation of time, min. |
| *h* | Hour angle, Deg. |
| *I* | Solar irradiance, W/m$^2$ |
| *LL* | Local longitude, Deg. |
| *LST* | local standard time, Min. |
| *L* | Local latitude, Deg. |
| *m* | Mass flow rate, kg/s |
| *N* | Day of the year |
| *SL* | Standard longitude, Deg. |

| | |
|---|---|
| *T* | Temperature, °C |
| *Ti* | Fluid inlet receiver temperature, °C |
| *To* | Fluid outlet receiver temperature, °C |
| *Z* | Solar azimuth angle, Deg. |
| ***Greek Symbols*** | |
| $\eta$ | Thermal efficiency, % |
| $\alpha$ | Solar altitude angle |
| $\delta$ | Solar declination angle |

## References


1. Zou, B.; Dong, J.; Yao, Y.; and Jiang, Y. (2016). An experimental investigation on a small-sized parabolic trough solar collector for water heating in cold areas. *Applied Energy*, 163, 396-407.
2. Bakos, G.C.; Ioannidis, I.; Tsagas, N.F.; and Seftelis, I. (2001). Design, optimisation and conversion-efficiency determination of a line-focus parabolic-trough solar-collector (PTC). *Applied energy*, 68(1), 43-50.
3. Palavras, I.; and Bakos, G.C. (2006). Development of a low-cost dish solar concentrator and its application in zeolite desorption. *Renewable Energy*, 31(15), 2422-2431.
4. Sakhare, V.; and Kapatkar, V.N. (2014). Experimental analysis of parabolic solar dish with copper helical coil receiver. *International Journal of Innovative Research in Advanced Engineering*, 1(8), 199-204.
5. Mohammed, I.L. (2012). Design and development of a parabolic dish solar water heater. *International Journal of Engineering Research and Applications*, 2(1), 822-830.
6. Al-Dohani, N.S.; Nayak, N.S.; Anarghya, A.; and Abhishek, V.N. (2018). Development of powerhouse using fresnel lens. *Proceeding of the International Conference on Research in Mechanical Engineering Sciences*. Manipal, Karnataka, India.
7. Valmiki, M.M.; Li, P.; Heyer, J.; Morgan, M.; Albinali, A.; Alhamidi, K.; and Wagoner, J. (2011). A novel application of a fresnel lens for a solar stove and solar heating. *Renewable Energy*, 36(5), 1614-1620.
8. Tripanagnostopoulos, Y.; Siabekou, C.; and Tonui, J.K. (2007). The fresnel lens concept for solar control of buildings. *Solar Energy*, 81(5), 661-675.
9. Lin, M.; Sumathy, K.; Dai, Y.J.; and Zhao, X.K. (2014). Performance investigation on a linear fresnel lens solar collector using cavity receiver. *Solar energy*, 107, 50-62.
10. Soriga, I.; and Neaga, C. (2012). Thermal analysis of a linear fresnel lens solar collector with black body cavity receiver. *International Journal of Low-Carbon Technologies*, 74(4), 106-116.
11. Nia, M.H.; Nejad, A.A.; Goudarzi, A.M.; Valizadeh, M.; and Samadian, P. (2014). Cogeneration solar system using thermoelectric module and fresnel lens. *Energy Conversion and Management*, 84, 305-310.
12. Perini, S.; Tonnellier, X.; King, P.; and Sansom, C. (2017). Theoretical and experimental analysis of an innovative dual-axis tracking linear fresnel lenses concentrated solar thermal collector. *Solar Energy*, 153, 679-690.

13. Xie, W.T.; Dai, Y.J.; and Wang, R.Z. (2011). Numerical and experimental analysis of a point focus solar collector using high concentration imaging PMMA fresnel lens. *Energy Conversion and Management*, 52(6), 2417-2426.
14. Eidan, A.; Al Sahlani, A.; and Obaid, A. (2020). Fresnel lens solar concentrator to utilize the extreme solar intensity in solar still receivers. *Proceeding of the Second International Scientific Conference of Al-Ayen University*. Thi-Qar, Iraq.
15. Kalogirou, S.A. (2014). *Solar energy engineering processes and systems* (2nd ed.). United Kingdom: Academic Press.
16. Abernethy, R.B.; Powel, D.B.; Colbert, D.; Sanders, D.G.; and Thompson, J.W. (1973). *Handbook, uncertainty in gas turbine measurements*. (AEDC-TR-73-5), AEDC Technical Library.
17. Hachim, D.M.; Alsahlani, A.; and Eidan, A.A. (2017). Measurements of wind and solar energies in Najaf, Iraq. *Advances in Natural and Applied Sciences*, 11, (9), 110-116.